General Disclaimer

One or more of the Following Statements may affect this Document

- This document has been reproduced from the best copy furnished by the organizational source. It is being released in the interest of making available as much information as possible.

- This document may contain data, which exceeds the sheet parameters. It was furnished in this condition by the organizational source and is the best copy available.

- This document may contain tone-on-tone or color graphs, charts and/or pictures, which have been reproduced in black and white.

- This document is paginated as submitted by the original source.

- Portions of this document are not fully legible due to the historical nature of some of the material. However, it is the best reproduction available from the original submission.

Produced by the NASA Center for Aerospace Information (CASI)

QUARTERLY REPORT NO. 2

1 March - 31 May 1969

NASA RESEARCH GRANT NGR-22-011-037

SUPPLEMENT NO. 4

INTER-RELATIONS BETWEEN ADVANCED PROCESSING TECHNIQUES,

INTEGRATED CIRCUITS, MATERIALS DEVELOPMENT AND ANALYSIS

by

B.L. Cochrun

W. Carlson

S. Fine

W.B. Nowak

NORTHEASTERN UNIVERSITY

BOSTON, MASSACHUSETTS

SECTION I
ACTIVE INTEGRATED CIRCUITS
B. Cochrun - W. Carlson

A 455 kHz i.f. amplifier using gyrator tuned circuits
has been built. The amplifier shown in the schematic
diagram of Figure 1 has two gyrator-amplifier stages
connected in cascade. The gyrator-amplifiers are a var-
iation of circuits described in earlier reports made
under this grant, particularly in Report No. 6, January
1, 1968, pp. 34 - 37, and Scientific Report of 1 January
1969, pp. 5 - 7. In these circuits the same transistors
are used as a gyrator resonator and to provide gain as an
amplifier.

A schematic diagram of the type of gyrator-amplifier used
in the i.f. amplifier is shown in Figure 2. The basic
gyrator circuit is that of Sipress and Witt[1]. Transistors
Q_1, Q_2, and Q_3, are part of the gyrator; Q_4 and Q_5 are cur-
rent sources of biasing the gyrator; and Q_6 is an emitter
follower. This method of biasing uses transistors of
both polarity types, usually a disadvantage in integrat-
ed circuits, but current source transistors do not have
to be of high quality and the lateral type transistor[2]
would be suitable. There are several other ways of
biasing the gyrator: Q_4 and Q_5 could be replaced by
field effect transistors operated as current sources
as shown in Figure 5, Scientific Report of 1 January 1969,
pp. 20 or one of two methods allowing the use of

transistors of the same polarity type as used in the
gyrator proper could be employed. These are the feed-
back scheme using transistors and breakdown diodes as
shown in Figure 5, page 21, and the two terminal current
source of Figures 11 and 12 in Scientific Report of
1 January 1969, pages 27 - 28, operation of which is
described on pages 11-14. The several methods of
biasing should ease the task of realizing the circuit
in integrated form.

The purpose of resistor R_f is to enhance the Q of the
gyrator by introducing at each port a negative cond-
uctance term to diminish the real parts of the short
circuit input admittances and thereby increase the Q.
If the T network of resistors connecting the emitters
of the first three transistors is converted to an equi-
valent delta network, it is seen that the gyrator is
equivalent to the gyrator of Figure 3, Scientific Report
of 1 January 1969, pp. 19 and described on pages 4 and 5.
For a gyrator of this kind, the maximum Q is equal to one-
half of the geometric mean of the beta's of transistors Q_1
and Q_3 if the current sources are ideal, but since
they are not, the Q will be somewhat less. If the
Q is less than desired, it may be increased by means of
R_f; if the Q is greater than desired, it may be decreased
by placing a conductance in shunt with one of the ports.

The voltage gain of the resonant amplifier at the
resonant frequency is approximately

$$V. \ G. = Q \ (R_e/R_{E1}) \ (R_2 C_2/R_1 C_1)^{1/2},$$

where R_1 is the sum of R_{1a} and R_{1b}, and it is assumed
that R_f is very much greater than R_1.

The bandwidth of the i.f. amplifier is 10 kHz. The Q of
each stage is 29.4. In the first stage of the amplifier
the transistors used gave a Q of about 16 requiring 82k
for R_f to increase the Q to the desired value. In the
second stage high beta transistors yielded a Q of about
50 requiring a 150 k resistor in shunt with one port of
the gyrator to reduce the Q. The two types of transistors
were used to illustrate the type of correction made to
increase or decrease gyrator Q. The voltage gain of the
amplifier is about 2,400.

_____

1. Sipress, J. M.; Witt, F. S., U. S. Patent 3,001,157,
September 19, 1961.

2. Lin, H. C.; Tan, T. B.; Chang, G. Y.; Van Der Leest,
B.; and Formigoni, N., Lateral Complementary Transistor
Structure for the Simultaneous Fabrication of Functional
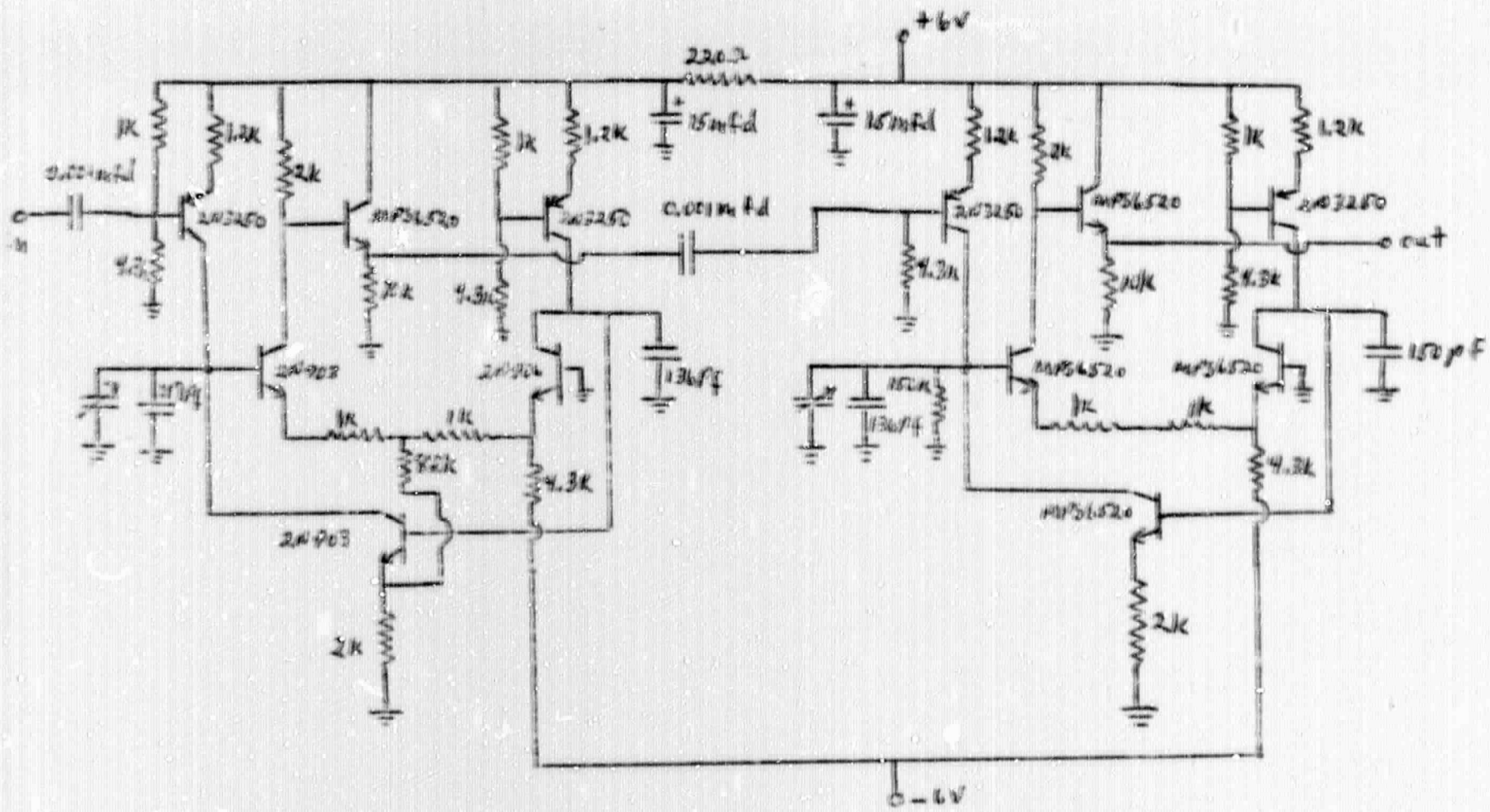Blocks, Proc. IEEE, Vol. 52, No. 12, pp. 1491-1495, Dec.
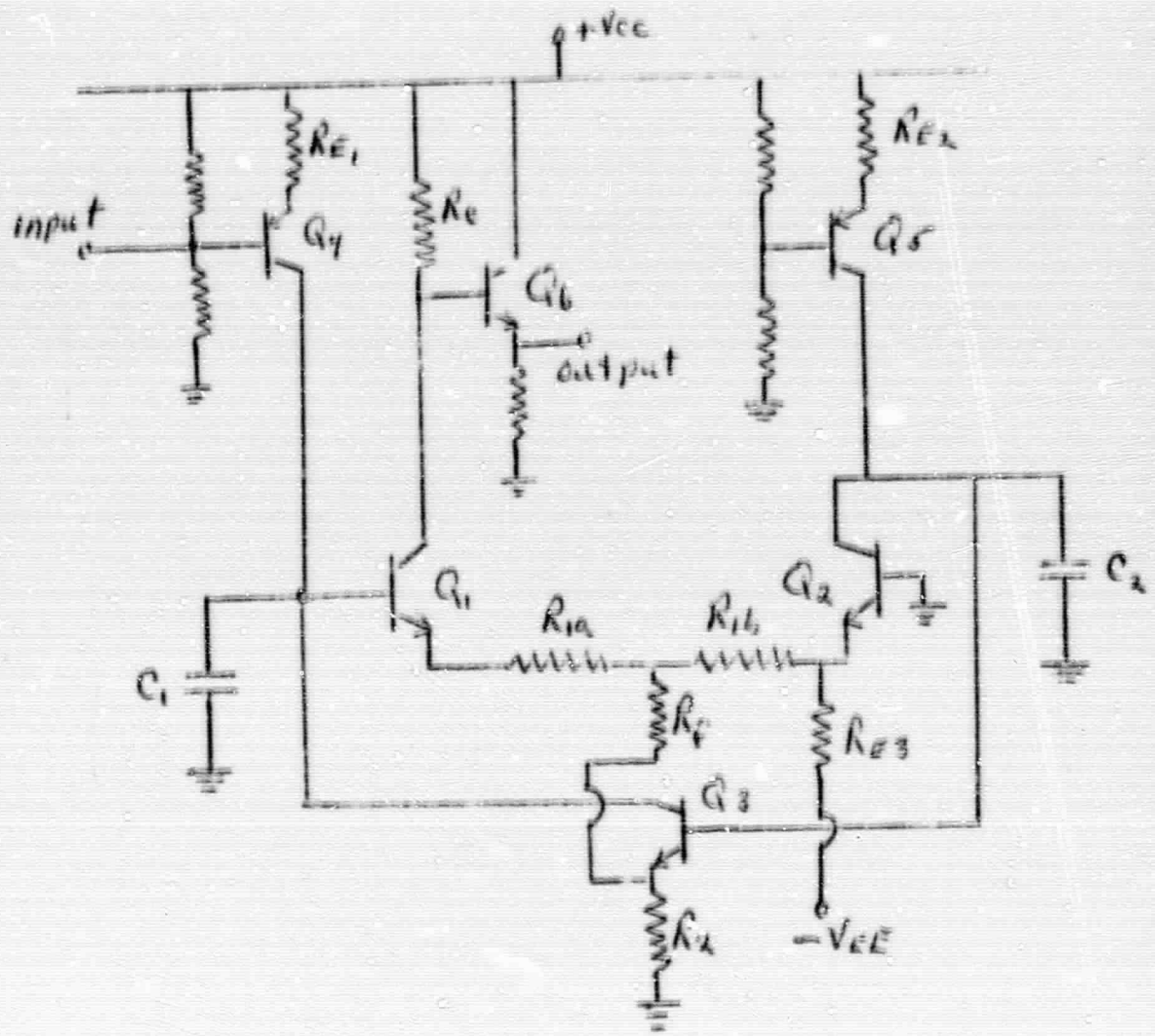1964.

FIGURE 1 455 kHz IF Amplifier

FIGURE 2   GYRATOR-AMPLIFIER CIRCUIT

SECTION II

METALLURGICAL STUDIES OF MICROCIRCUIT INTERCONNECTIONS

W. B. Nowak   T. Hull   P. Salmon

It is convenient to describe the efforts of this quarter under three items:

  1. Calibration of reflectivity measurements with a reflectance standard, and precision of these measurements.

  2. Reflectivity measurements on Au/Pt film couples on glass.

  3. Analytical macroscopic solution of the diffusion problem.

(1) A comparison was made between the spectral reflectance of AU films and bulk Au (literature values) using a fresh MgO standard prepared in the manner described in Quarterly Report No.1. Agreement with ±10% was obtained. Reproducibility (precision) of our reflectivity measurements is a few percent.

However, subsequent measurements on Au films did not give the same agreement with bulk values, especially at λ=633 millimicrons. It was then discovered that the MgO standard had degraded in the laboratory environment over a period of several days. Fresh MgO standards had to be prepared for each day's reflectance measurements. Another problem with these MgO standards was their lack of cohesiveness, so that they could not be used in the inverted position to obtain calibrations

through the glass slide (substrate). These considerations led
to the use of Eastman Kodak "white reflectance paint" which
is stable in air, very cohesive and durable, and is "white"
for $350 < \lambda < 800$ millimicrons. This paint will be our
standard instead of MgO for all future work.

(2) Reflectivity measurements have been made on Au, Pt, and
Au-on-Pt films on glass substrates. Most of the work reported
here is from the thesis submitted by Thomas Hull to Northeastern
University in partial fulfillment of the requirements for the
degree of Master of Science.

Au-on-Pt thin film couples were deposited on Corning 7059
glass microscope slides by thermal evaporation from tungsten
filaments at about 10^{-5} torr. The glass substrates were held
at 200°C for the Pt deposition and were allowed to cool to
ambient temperature for the Au deposition (to inhibit diffusion
during the evaporation procedures). Regions of pure Au and pure
Pt were deposited on the same substrate and in the same pump-
down cycle as the Au/Pt couples by means of a spring-loaded
two-position mask. These single-neutral regions were used
for electrical resistivity, reflectivity, and film thickness
comparisons.

Approximate calculations using bulk values for Q and E in the
expression for the diffusion coefficient, $D=D_0 e^{-E/rt}$, in-
dicated that an observable reflectance change might be expected
after 1/2 hour at 500°C for a 6000 $\overset{\circ}{A}$ Au film, viewed from the
Au side. Exploratory reflectance measurements were made after

each of series of heat treatments for one hour at 30°C intervals from 350° - 700°C. These heat treatments resulted in the formation of blisters in the region of the Au/Pt couple at temperatures greater than about 200°C. New specimens were fabricated with a thin tantalum oxide underlayer next to the substrate in an attempt to reduce the blistering. The improvement was marginal.

Samples were fabricated and tested for spectral reflectivity as a function of heat treatment for Pt thicknesses ranging from $250 \overset{\circ}{A}$ to $1250 \overset{\circ}{A}$ and Au thicknesses ranging from 4000 to $6000 \overset{\circ}{A}$. The thinness of the Pt films was due to the difficulty in obtaining thicker films using thermal evaporation from tungten filaments. In the future, electron beam evaporation will be used, although this will introduce other variations in the nature of the films deposited. Heat treatments were carried out at 675°C for one hour increments. A typical set of reflectivity results is given in Figs. 1 and 2 for the Pt side (viewed through the glass substrate). Various changes occurred that ceased after four hours, although no definite trends could be discerned from the limited data. Figures 3 and 4 present the spectral reflectivity of the Pt and Au standards associated with the Au/Pt couple of Figs. 1 and 2. The Pt film showed a dramatic increase in reflectivity after one hour, whereas the Au film showed a slight decrease in reflectivity, with some shifts of the spectral curve in both cases. Figure 3 is a graph of the reflectivity (at 490 mμ) of Au, Pt, and the Pt side of the Au/Pt couple as a function of annealing temperature. In this sample, the Au decreased markedly and the Pt increased markedly

These unexpected changes may have obscured those expected due to diffusion, and this matter is under investigation.

The following table presents the reflectivity and room temperature resistivity of a Au/Pt couple and accompanying Au and Pt films for 1250 Å of Pt and 5500 Å of Au before and after annealing for one hour at $675^{\circ}C$.

	Reflectivity (490 mμ) (Arbitrary Units)		Elec. Resist. (room Temp.) (microhm - cm)		
Specimen	Initial	Final	Initial	Final	Bulk
Au	290	250	2.7	2.7	2.44
Pt	62	152	90	20.3	10.5
Pt side of Au/Pt	60	200	----	----	

The electrical resistivity values indicate that the films were probably continuous, but that the Pt film contained a high density of defects, with a low density of defects in the Au film. Although the thin Pt films were not optically dense, the reflectivity of the Pt film through the glass matched that of the Pt in the Au/Pt couple. This result is supported by the theoretical curve for Pt reflectivity versus film thickness (O.S. Heavens, Optical Properties of Thin Solid Films, Dover Pub. Co., N.Y. 1965, p. 261). Thus, it appears that the increase in reflectivity and decrease in resistivity of the Pt may be caused by a recrystallization of the film even at this low temperature. (Gold has been reported to recrystallize as low as $150^{\circ}C$.)
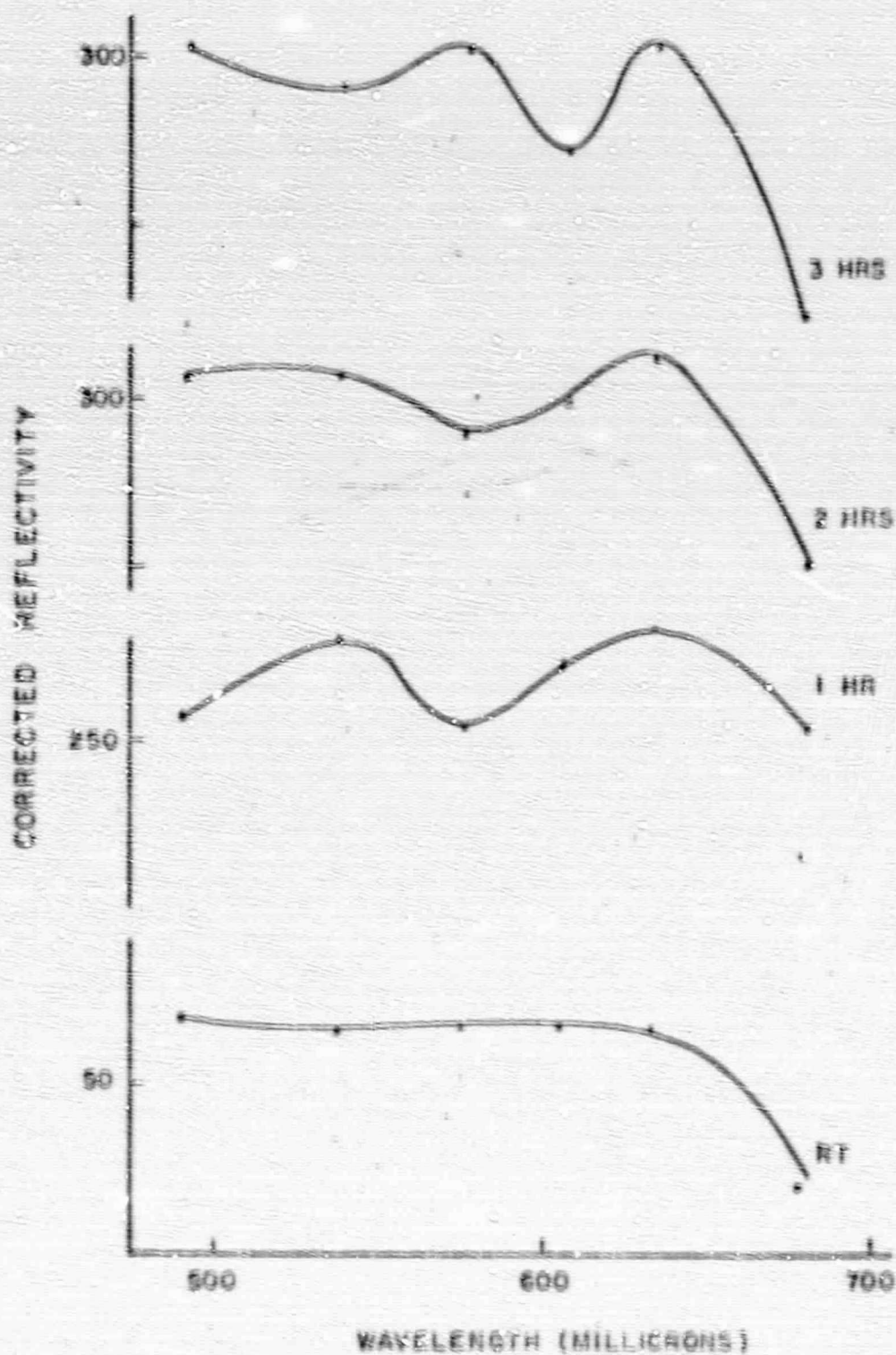
This model would apply to systems with complete solid solubility and a diffusion constant which is independent of composition.

Work for the next quarter will continue to the reflectivity of Au, Pt, and Au/Pt films with reference to then possible recrystallization and diffusion.

REFLECTIVITY VS WAVELENGTH
FOR
ANNEALING TIMES AT 675°C
(SAMPLE 5C)

FIGURE 1

REFLECTIVITY VS WAVELENGTH
FOR
ANNEALING TIMES AT 675°C
(SAMPLE 5C)

CORRECTED REFLECTIVITY

7 HRS

6 HRS

5 HRS

4 HRS

WAVELENGTH (MILLIMICRONS)
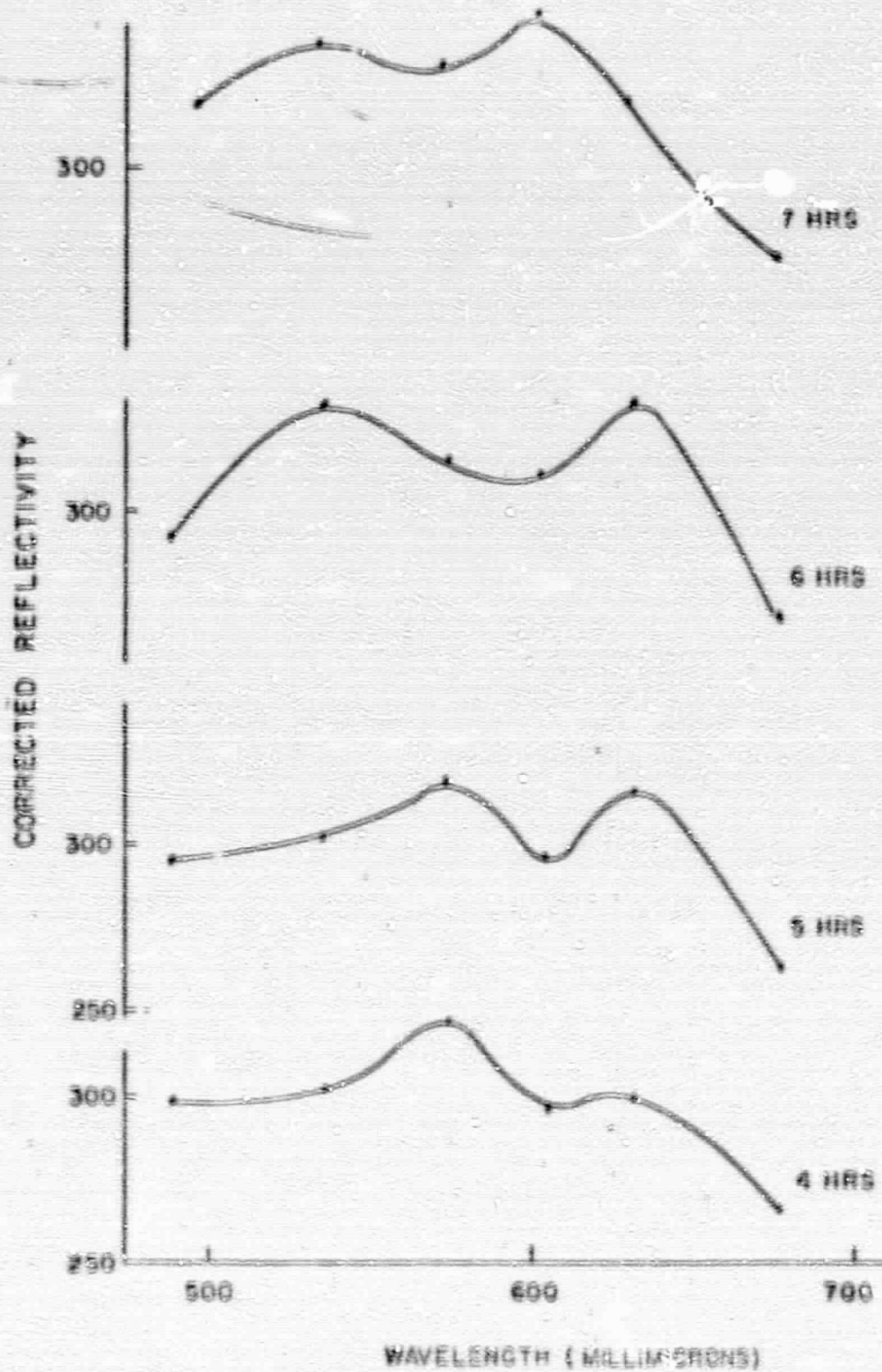
FIGURE 2

REFLECTIVITY VS WAVELENGTH
FOR
5C PLATINUM STANDARD
(ANNEALED AT 675°C)
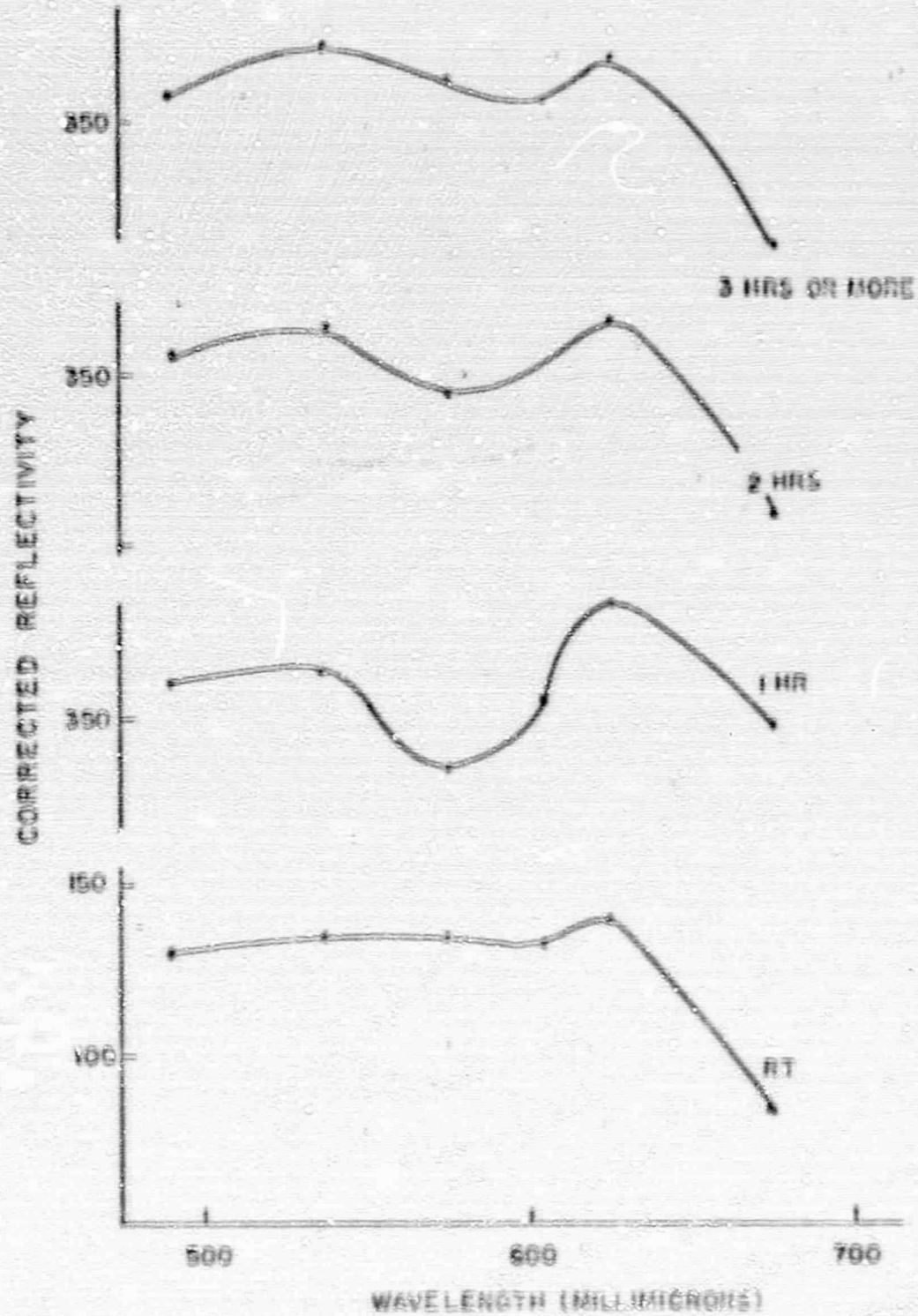
FIGURE 3

REFLECTIVITY VS WAVELENGTH
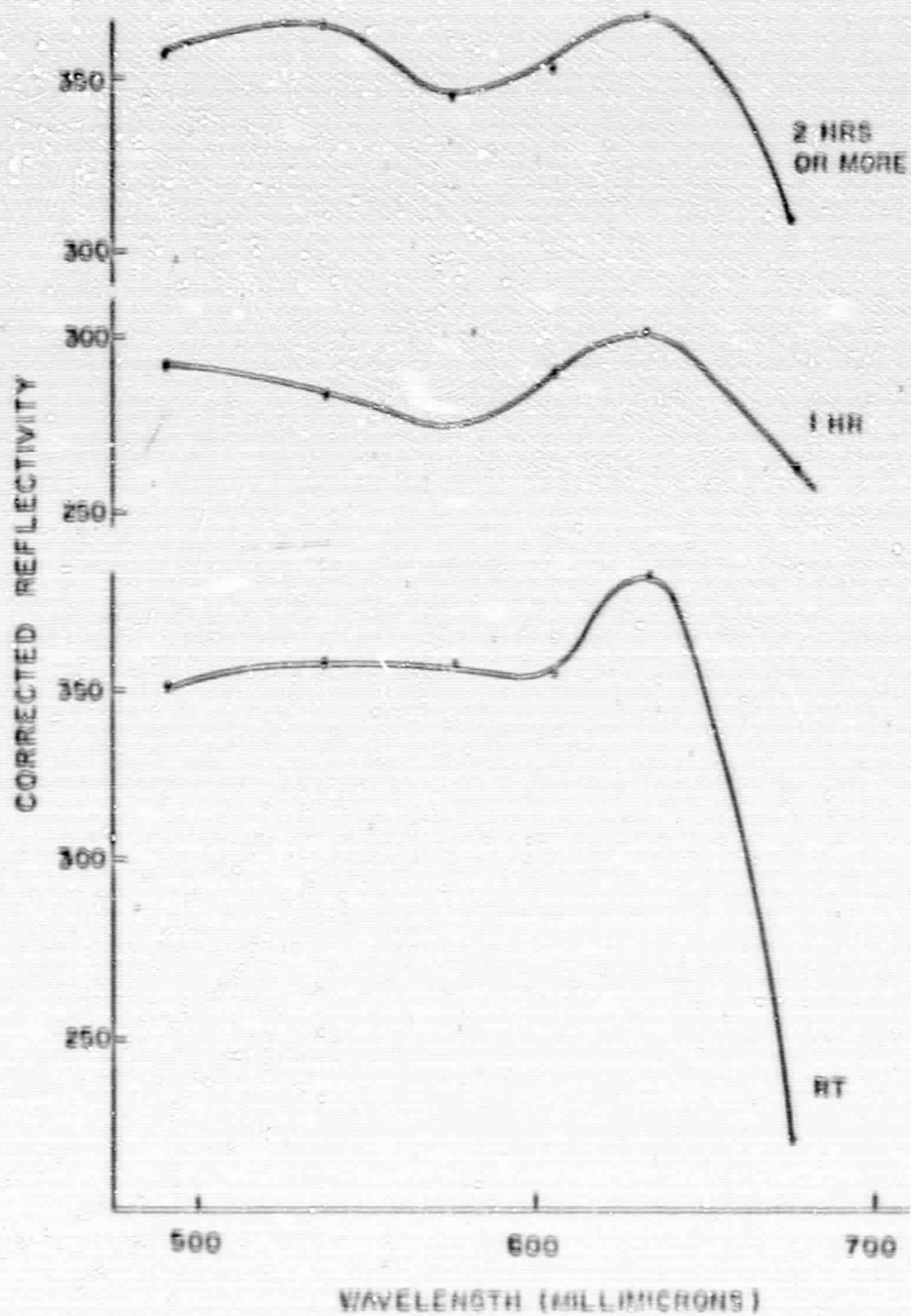
FOR

SC GOLD STANDARD

(ANNEALED AT 675° C)

FIGURE 4

REFLECTIVITY VS ANNEALING TEMPERATURE

(ANNEALED FOR 1 HOUR AT EACH
PROGRESSIVELY HIGHER TEMPERATURE)

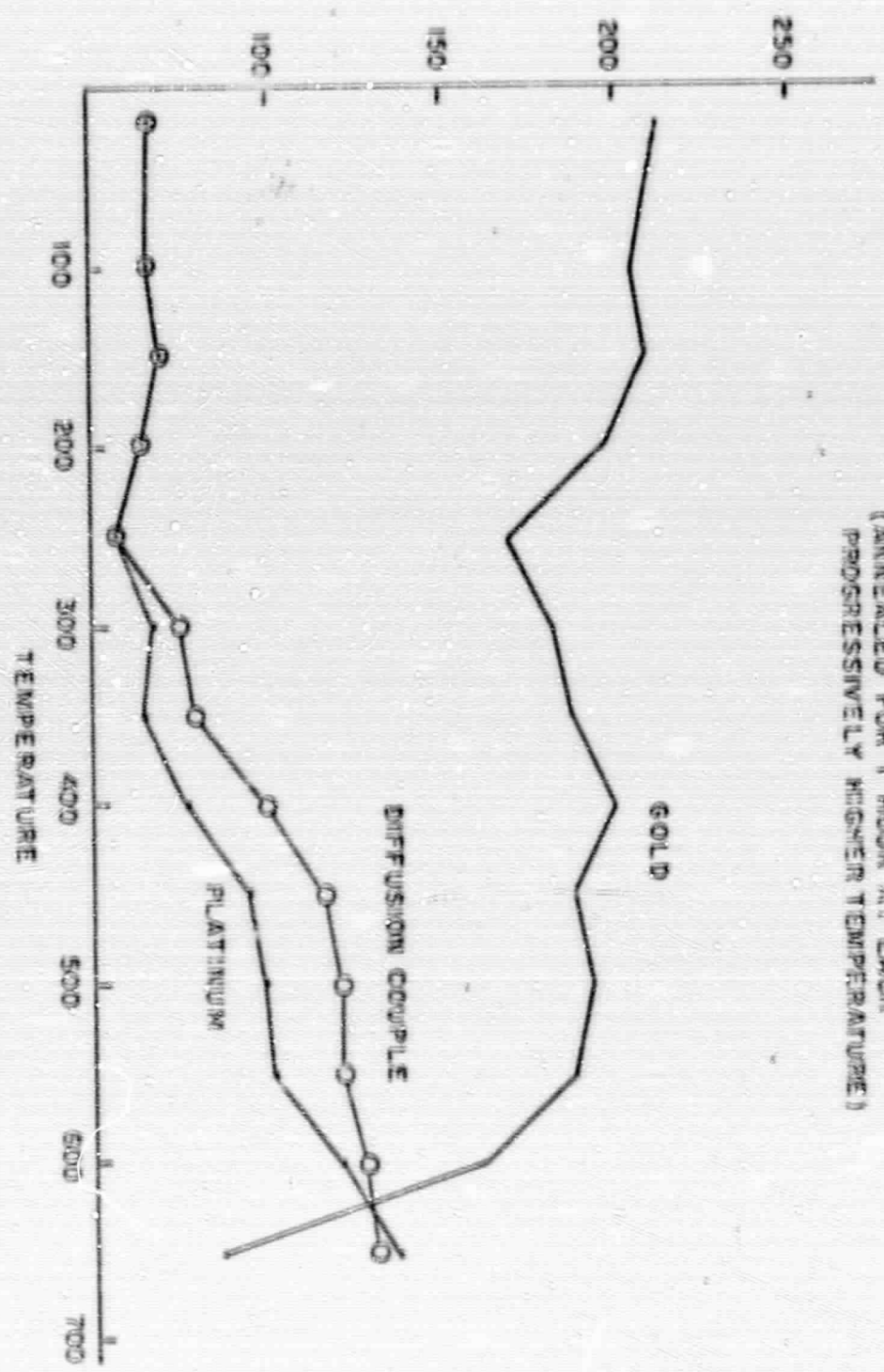FIGURE 5

The solution to the finite slab with insulated faces and initial temperature distribution is taken from Carslaw and Jaeger, p. 101.[47]

$$v = \frac{1}{L}\int_0^L f(x')dx + \frac{2}{L}\sum_{n=1}^{\infty}\left[e^{-\frac{kn^2\pi^2 t}{L^2}}\cos\frac{n\pi x}{L}\int_0^L f'(x)\cos\frac{n\pi x'}{L}dx'\right]$$

where $f(x')$ = initial temperature distribution

v = temperature

L = total thickness

k = heat transfer coefficient

t = time .

The diffusion analogy is:

$$C = \frac{1}{L}\int_0^L f(x')dx + \frac{2}{L}\sum_{n=1}^{\infty}\left[e^{-\frac{Dn^2\pi^2 t}{L^2}}\cos\frac{n\pi x}{L}\int_0^L f(x')\cos\frac{n\pi x'}{L}dx'\right]$$

where C = composition

D = diffusion constant .

To approximate the multicomponent film, the initial distribution is:

$$f(x') = C_c, \qquad 0 < x < h$$

Appendix B - 2

$$f(x') = 0, \qquad h < x < L \quad .$$

Thus, the integrals become:

$$\int_0^L f(x')dx = \int_0^h C_0 dx' + 0 = hC_0$$

and

$$\int_0^L f(x')\cos\frac{n\pi x'}{L}dx' = \int_0^h C_0 \cos\frac{n\pi x'}{L}dx' + 0 = \frac{C_0 L}{n\pi} \sin\frac{n\pi h}{L} \quad .$$

The solution becomes:

$$C = \frac{hC_0}{L} + \frac{2C_0}{\pi} \sum_{n=1}^{\infty} \left[\frac{1}{n} e^{-\frac{Dn^2\pi^2 t}{L^2}} \cos\frac{n\pi x}{L} \sin\frac{n\pi h}{L} \right]$$

$$\frac{C}{C_0} = \frac{h}{L} + \frac{2}{\pi} \sum_{n=1}^{\infty} \left[\frac{1}{n} e^{-\frac{Dn^2\pi^2 t}{L^2}} \cos\frac{n\pi x}{L} \sin\frac{n\pi h}{L} \right] \quad .$$

If we consider a surface analysis, then

$$x = 0$$

and the solution reduces to:

$$\frac{C}{C_0} = \frac{h}{L} + \frac{2}{\pi} \sum_{n=1}^{\infty} \frac{1}{n} e^{-\frac{Dn^2\pi^2 t}{L^2}} \sin\frac{n\pi h}{L} \quad .$$

Biophysical Studies

S. Fine

The following is a summary of progress during the past three
months relating to the grant.

1.   Publications

a.   Laor, Y., Simpson, C. L., Klein, E., and Fine, S., "Pathology of
     Internal Viscera Following Laser Radiation," American Journal of the
     Medical Sciences, Vol. 257, April 1969.

2.   Presentations

a.   Fine, S., "The Application of Lasers to Biology and Medicine,"
     Conference on Trends and Directions in Biological Sciences of the
     Thirteen Colleges Curriculum Program Biology Teachers, Clark Col-
     lege, Atlanta, Georgia, March 1969.

b.   S. Fine - Participation in Skin Laser Workshop, Second International
     Laser Safety Conference, Cincinnati, Ohio, March 1969.

c.   Fine, S., Lasers - Characteristics, Uses, Hazards, and Biological
     Effects, Seminar Series, Environmental Health Engineering and Sci-
     ence, Graduate School of Engineering, Northeastern University,
     March 1969.

d.   Fine, S., Lasers - Characteristics and Uses in Biology and Medicine,
     Surgical Seminar Series, Boston University School of Medicine, March
     1969.

e.   Fine, S., Use of Lasers in Biology and Medicine, Laser Applications
     Course, Washington University, St. Louis, Missouri, May 1969.

3. Laser and Related Studies

The manuscript on pressure and temperature in the anterior aqueous chamber on CO_2 irradiation has been completed and is being prepared for submission. Studies have been initiated on the temperature elevation for threshold injury to the eye on CO_2 irradiation. Initial calculations have been carried out on hazards associated with incoherent narrow beam divergence and semiconductor laser irradiation.

4. Rupture and Tensile Strength Measurements of Fresh and Treated Canine Aortic Tissue

Rupture and tensile strength measurements have been carried out on longitudinal samples. The relative strength of longitudinal specimens to transverse specimens is dependent on the position along the aorta. Calculations are being carried out to determine in which regions of the aorta it can be considered as a thin-walled cylinder.

5. Flow Measurements on an Experimental Aortic-Pulmonary Shunt

Flow studies are being conducted on a shunt created between the aorta and right pulmonary artery. Square wave electromagnetic flowmeters are placed around the aorta proximal distal to the shunt to measure flow. The flow through the shunt is the difference in flow as measured as a function of hematocrit, and after administration of epinephrine and isoproterenol.